Charge transfer in low-energy collisions of He^{2+} and Li^{3+} with various neutral atoms

Mark T. Stollberg and Hai-Woong Lee
Department of Physics, Oakland University, Rochester, Michigan 48063
(Received 6 December 1983)

Charge-transfer cross sections for He^{2+} and Li^{3+} colliding with H, He, Li, Be, B, C, Ne, Na, Mg, Ar, K, Ca, and Cs have been calculated using the Landau-Zener model over the velocity range 10^7–10^8 cm/sec. In these collisions, electron capture occurs predominantly into excited states of the product ion, He^{2+} or Li^{2+}. Laser-gain calculations have also been made for consideration of a possible short-wavelength laser.

I. INTRODUCTION

It has been proposed[1,2] that charge-transfer processes may serve as a means of achieving population inversion for short-wavelength (vuv and soft-x-ray) lasers. Some selected charge-transfer processes of multiply charged ions, in particular, have large cross sections necessary to meet the high-gain requirement of a short-wavelength laser. In addition, these processes often involve crossings of potential energy surfaces and thus offer an opportunity to be described by the simple Landau-Zener model.[3,4] Although not very accurate, charge-transfer cross sections obtained by the Landau-Zener model can be used for a preliminary screening of likely candidate processes for short-wavelength lasers.

In this work Landau-Zener cross sections for electron transfer from neutral atoms to He^{2+} and Li^{3+} ions are calculated over the ion velocity range 10^7–10^8 cm/sec. The atoms considered are H, He, Li, Be, B, C, Ne, Na, Mg, Ar, K, Ca, and Cs. Electrons transferred from these atoms populate predominantly the first few excited states of He^+ ($n=2,3$) and Li^{2+} ($n=2,3,4$). For the case of He^+, the Lyman-α, Lyman-β, and Balmer-α transitions would result with $\lambda=30.4$, 25.6, and 165 nm, respectively. In Li^{2+} the Lyman-α, -β, and -γ transitions, Balmer-α and -β transitions, and Paschen-α transitions may occur. Corresponding wavelengths are 13.5, 11.4, 10.8, 72.9, 54.0, and 208 nm.

In Sec. II a brief review of the Landau-Zener model is given. In Sec. III the result of our cross-section and gain calculations are presented. Analysis of our data and discussion are given in Sec. IV.

II. THEORY

The Landau-Zener model[3,4] represents perhaps the simplest means of describing nonadiabatic transition at the crossing of potential energy surfaces. Although its limitations are well known,[5–7] the model continues to be used for a rough estimate of cross sections associated with various collision processes.[8–10] Here we briefly describe the model as it is applied to charge-transfer processes of multiply charged ions.

Let us consider a charge-transfer process

$$A+B^{Z+}\rightarrow A^{+}+B^{(Z-1)+}\ . \tag{2.1}$$

At large internuclear distance R, the potential energy curves for the initial and final configurations are given, respectively, by

$$H_i(R)\cong\Delta E-\frac{Z^2e^2\alpha(A)}{2R^4}\ , \tag{2.2a}$$

$$H_f(R)\cong\frac{(Z-1)e^2}{R}-\frac{(Z-1)^2e^2\alpha(A^+)}{2R^4}-\frac{e^2\alpha(B^{(Z-1)+})}{2R^4}\ . \tag{2.2b}$$

Here we have assumed spherically symmetric states and consequently neglected $1/R^3$ terms in the potential. ΔE is the defect energy and α denotes the polarizability of the atom or ion being considered. If $\Delta E>0$, the two curves cross at $R=R_c$ where R_c satisfies

$$\frac{(Z-1)e^2}{R_c}=\Delta E-\frac{Z^2e^2\alpha(A)}{2R_c^4}+\frac{(Z-1)e^2\alpha(A^+)}{2R_c^4}+\frac{e^2\alpha(B^{(Z-1)+})}{2R_c^4}\ . \tag{2.3}$$

In the Landau-Zener model one assumes that the transition (electron transfer in our case) is limited to a narrow region around the crossing point R_c. One further assumes that in this narrow region the potential energy separation varies linearly with the internuclear distance,

$$H_i-H_f\cong\gamma(R-R_c)\ , \tag{2.4}$$

and the coupling matrix element H_{if} is a constant,

$$H_{if}\cong\beta\ . \tag{2.5}$$

The constant γ can easily be computed for our case of charge transfer using Eqs. (2.2),

$$\gamma=\frac{(Z-1)e^2}{R_c^2}+\frac{4Z^2e^2\alpha(A)}{2R_c^5}-\frac{4(Z-1)^2e^2\alpha(A^+)}{2R_c^5}-\frac{4e^2\alpha(B^{(Z-1)+})}{2R_c^5}\ . \tag{2.6}$$

For the coupling H_{if} we use the formula suggested by Ol-

 ©1984 The American Physical Society

son, Smith, and Bauer,[11]

$$H_{if}=\beta=\tfrac{1}{4}\epsilon_i\epsilon_f(\epsilon_i+\epsilon_f)R_c\exp[-0.43(\epsilon_i+\epsilon_f)R_c] . \quad (2.7)$$

All quantities in Eq. (2.7) should be expressed in atomic units, and ϵ_i and ϵ_f are determined by $\epsilon_i=\sqrt{2I_i}$ and $\epsilon_f=\sqrt{2I_f}$, where I_i and I_f are the effective ionization potentials (in atomic units) of the electron before and after the transfer, respectively.

The Landau-Zener transition probability as the system passes by the crossing point twice in a collision process is given by

$$P=2\exp(-p)[1-\exp(-p)] , \quad (2.8)$$

where

$$p=\frac{2\pi\beta^2}{\hbar v\gamma\left[1-\left[\frac{b}{R_c}\right]^2\right]^{1/2}} , \quad (2.9)$$

b is the impact parameter, and v is the velocity of the ion at the crossing point, which is virtually the same as the initial ion velocity for all the processes we consider for the velocity $v\gtrsim 10^7$ cm/sec. The integration of the probability P with respect to the impact parameter b yields the well known expression[8] for the Landau-Zener cross section,

$$\sigma=4\pi R_c^2[E_3(\eta/v)-E_3(2\eta/v)] , \quad (2.10)$$

where

$$\eta=\frac{2\pi\beta^2}{\hbar\gamma} , \quad (2.11)$$

and the exponential integral E_3 is defined as[12]

$$E_3(x)=\int_1^\infty \frac{dz}{z^3}\exp(-xz) . \quad (2.12)$$

For collision processes we consider, electron capture occurs predominantly into excited states of the product ion $B^{(Z-1)+}$, producing population inversion between two levels of the ion. Assuming the system is Doppler broadened, the gain g is then given by[13]

$$g=\sqrt{\pi\ln 2}\frac{\lambda^2\Delta N}{8\pi\tau_s\Delta\nu} , \quad (2.13)$$

where $\Delta\nu$ and λ are, respectively, the linewidth and wavelength of the transition in question, τ_s is the spontaneous lifetime of the upper level, and ΔN is the inversion density

$$\Delta N=N_2-N_1\frac{g_2}{g_1} . \quad (2.14)$$

Subscripts 1 and 2 refer to the lower and upper laser levels, respectively, g_i is the degeneracy of the ith level, and N_i is the number density of the product ion in the ith level. N_1 and N_2 are determined by charge-transfer cross sections into the lower and upper levels σ_1 and σ_2 as

$$N_1=N_{AZ+}N_B\sigma_1 v\tau_s , \quad (2.15a)$$

$$N_2=N_{AZ+}N_B\sigma_2 v\tau_s . \quad (2.15b)$$

Here N_{AZ+} and N_B are number densities of the ion A^{Z+} and atom B.

III. RESULT OF CALCULATION

Our calculation of the Landau-Zener charge-transfer cross section was carried out in the following steps.

(1) The crossing distance R_c was calculated from Eq. (2.3). The polarizabilities α were obtained from two sources.[14,15] Polarizabilities for He^{2+} and Li^{3+} are less than 0.005 Å^3 and so were taken to be zero. Because of the limitation of the Landau-Zener model, only those processes for which the crossing distance satisfies $2\le R_c\le 10$ Å were considered. This excludes the important reaction $He^{2+}+Li\rightarrow He^+(n=3)+Li^+$. The same process with the product ion in the $(n=2)$ level was included in our calculation.

(2) The constants γ and β were calculated from Eqs. (2.6) and (2.7) and were used to evaluate η defined by Eq. (2.11).

(3) Once R_c and η are known, the cross section σ can easily be calculated from Eq. (2.10) for different values of the ion velocity v. A standard mathematical handbook[12] contains a table of the function $E_3(x)$. However, we find it more convenient to directly compute the integral. For this purpose we rewrite Eq. (2.10) as

$$\sigma=4\pi R_c^2\int_0^1 y\,dy[\exp(-\eta/vy)-\exp(-2\eta/vy)] . \quad (3.1)$$

Equation (3.1) was then numerically integrated using a six-point Gauss-Legendre quadrature.

The result of our calculation is summarized in Table I for helium and in Table II for lithium reactions. Shown in the tables are the peak cross section σ_{max}, the velocity v_{max} at which the peak cross section occurs, and the half-width at half maximum w of the σ-vs-v curve, in addition to polarizabilities α, the energy defect ΔE, the crossing distance R_c, the coupling matrix element β, and the parameter η. Since the σ-vs-v curve is, in general, not symmetric about the peak, we have defined the width to the left and right of the peak, w_L and w_R, separately. A bracket is used to denote a process for which the peak cross section occurs beyond the velocity range 10^7–10^8 cm/sec. For such a process, only one of the two widths is important, σ_{max} in the tables represents not the peak cross section but simply the largest value of the cross section in the velocity range 10^7–10^8 cm/sec, and v_{max} denotes the velocity at which this largest value of cross section is obtained. In both Table I and II the reactions are presented in an order of increasing η. The parameter η is important for our analysis to follow because, as will be shown in Sec. IV, this parameter determines the position and the width of the peak; v_{max}, and w_L and w_R.

Figures 1 and 2 are typical sets of σ-vs-v curves for helium and lithium reactions, respectively. We see that helium reactions generally have larger cross sections, indicating that charge-transfer processes of He^{2+} are generally preferred to those of Li^{3+} for consideration of a short-wavelength laser. This is further borne out by Fig. 3, in which the gain curves for He^{2+} with Be and Li, and Li^{3+} with H are shown. The gain was calculated from Eq. (2.13) assuming the Doppler width $\Delta\nu=10^{12}$ Hz, and the

TABLE I. Parameters for charge transfer between He^{2+} and various atoms. Parentheses are used to denote quantities associated with a process for which the peak cross section occurs beyond the velocity range 10^7–10^8 cm/sec.

Reaction	$\alpha(A)$ (Å^3)	$\alpha(A^+)$ (Å^3)	ΔE (eV)	R_c (Å)	β (eV)	η (10^5 cm/sec)	σ_{max} (Å^2)	v_{max} (10^7 cm/sec)	w_L (10^7 cm/sec)	w_R (10^7 cm/sec)
$He^{2+}+K\rightarrow He^+(n=3)+K^+$	43.40	0.95	1.747	9.167	0.0056	0.1206	(1.128)	(1.1)		(0.1)
$He^{2+}+Cs\rightarrow He^+(n=3)+Cs^+$	59.60	3.08	2.193	8.049	0.0170	0.6524	(4.556)	(1.1)		(0.1)
$He^{2+}+C\rightarrow He^+(n=2)+C^+$	1.760	0.82	2.326	6.269	0.0372	3.432	(12.94)	(1.1)		(0.3)
$He^{2+}+Cs\rightarrow He^+(n=2)+Cs^+$	59.60	3.08	9.697	4.072	0.2679	9.897	(12.48)	(1.1)		(0.9)
$He^{2+}+K\rightarrow He^+(n=2)+K^+$	43.40	0.95	9.251	3.872	0.3203	14.67	(14.49)	(1.1)		(1.5)
$He^{2+}+Li\rightarrow He^+(n=2)+Li^+$	24.30	0.300	8.200	3.594	0.4067	27.31	(16.69)	(1.1)		(2.6)
$He^{2+}+Na\rightarrow He^+(n=2)+Na^+$	23.60	0.15	8.452	3.530	0.4390	30.12	(16.60)	(1.1)		(2.0)
$He^{2+}+Ca\rightarrow He^+(n=2)+Ca^+$	25.00	8.34	7.479	3.687	0.7695	114.6	19.33	2.7	1.9	11.0
$He^{2+}+Be\rightarrow He^+(n=2)+Be^+$	5.600	1.81	4.270	3.940	0.5205	166.6	22.07	3.9	2.7	16.0
$He^{2+}+Mg\rightarrow He^+(n=2)+Mg^+$	10.60	3.32	5.946	3.513	0.8370	204.5	17.55	4.9	3.3	19.0
$He^{2+}+B\rightarrow He^+(n=2)+B^+$	3.030	1.53	5.294	3.172	1.0995	484.7	(14.19)	(9.9)	(6.3)	

inversion density was obtained with $N_{AZ+}=10^{16}$ cm^{-3} and $N_B=10^{16}$ cm^{-3}. The spontaneous lifetimes τ_s were obtained from Ref. 16. We obtain $\tau_s=1.3\times10^{-10}$ sec for the Lyman-α transition of He^{2+}, and $\tau_s=2.6\times10^{-11}$ sec for the Lyman-α transition of Li^{2+}. Overall, within the Landau-Zener model, the He^{2+}-Be reaction appears to offer the best chance for a short-wavelength laser. However, this observation was made under an unrealistic assumption that densities of ions and atoms available are the same regardless of the type of the ion or atom ($N_{AZ+}=10^{16}$ cm^{-3}, $N_B=10^{16}$ cm^{-3}). We also note that, for the He^{2+}-Li reaction, we only considered electron capture into the first excited level ($n=2$) of He^+. There exists, however, experimental[17] and theoretical[18,19] evidence that it is the second excited level ($n=3$) of He^+ that is predominantly populated in collisions of He^{2+} with Li. For this case the crossing distance R_c is too large for the Landau-Zener model to be reliable.

IV. ANALYSIS AND DISCUSSION

The general behavior of the Landau-Zener cross section with respect to the velocity is largely determined by the three quantities σ_{max}, v_{max}, and w (w_L and w_R). In this section we show that, within the Landau-Zener model, these three quantities are completely determined by the two parameters R_c and η.

TABLE II. Parameters for charge transfer between Li^{3+} and various atoms. Parentheses are used to denote quantities associated with a process for which the peak cross section occurs beyond the velocity range 10^7–10^8 cm/sec.

Reaction	$\alpha(A)$ (Å^3)	$\alpha(A^+)$ (Å^3)	ΔE (eV)	R_c (Å)	β (eV)	n (10^5 cm/sec)	σ_{max} (Å^2)	v_{max} (10^7 cm/sec)	w_L (10^7 cm/sec)	w_R (10^7 cm/sec)
$Li^{3+}+K\rightarrow Li^{2+}(n=4)+K^+$	43.40	0.95	3.280	9.708	0.0022	0.0106	(0.112 0)	(1.1)		(0.1)
$Li^{3+}+He\rightarrow Li^{2+}(n=2)+He^+$	0.00	0.204 956	5.998	4.793	0.0055	0.0232	(0.059 58)	(1.1)		(0.1)
$Li^{3+}+Be\rightarrow Li^{2+}(n=3)+Be^+$	5.60	1.81	4.251	6.989	0.0043	0.0266	(0.141 7)	(1.1)		(0.1)
$Li^{3+}+Cs\rightarrow Li^{2+}(n=4)+Cs^+$	59.60	3.08	3.726	9.082	0.0046	0.0340	(0.313 6)	(1.1)		(0.1)
$Li^{3+}+Cs\rightarrow Li^{2+}(n=3)+Cs^+$	59.60	3.08	9.678	5.422	0.0664	1.002	(3.141)	(1.1)		(0.1)
$Li^{3+}+Cs\rightarrow Li^{2+}(n=2)+Cs^+$	59.60	3.08	26.685	3.735	0.1592	1.084	(1.622)	(1.1)		(0.1)
$Li^{3+}+Mg\rightarrow Li^{2+}(n=3)+Mg^+$	10.60	3.32	5.927	5.469	0.0389	1.268	(3.179)	(1.1)		(0.1)
$Li^{3+}+K\rightarrow Li^{2+}(n=3)+K^+$	43.40	0.95	9.232	5.229	0.0772	1.458	(4.163)	(1.1)		(0.1)
$Li^{3+}+Ca\rightarrow Li^{2+}(n=3)+Ca^+$	25.00	8.34	7.460	5.187	0.0656	1.617	(4.511)	(1.1)		(0.1)
$Li^{3+}+B\rightarrow Li^{2+}(n=3)+B^+$	3.03	1.53	5.285	5.613	0.0299	1.667	(2.824)	(1.1)		(0.1)
$Li^{3+}+K\rightarrow Li^{2+}(n=2)+K^+$	43.40	0.95	26.239	3.524	0.2147	1.929	(2.448)	(1.1)		(0.1)
$Li^{3+}+Li\rightarrow Li^{2+}(n=3)+Li^+$	24.30	0.03	8.181	5.031	0.0851	2.237	(5.711)	(1.1)		(0.3)
$Li^{3+}+Na\rightarrow Li^{2+}(n=3)+Na^+$	23.60	0.15	8.433	4.927	0.0983	2.806	(6.701)	(1.1)		(0.3)
$Li^{3+}+Li\rightarrow Li^{2+}(n=2)+Li^+$	24.30	0.03	25.188	3.147	0.3512	5.053	(4.503)	(1.1)		(0.5)
$Li^{3+}+Na\rightarrow Li^{2+}(n=2)+Na^+$	23.60	0.15	25.440	3.115	0.3702	5.505	(4.725)	(1.1)		(0.5)
$Li^{3+}+Ca\rightarrow Li^{2+}(n=2)+Ca^+$	25.00	8.34	24.467	3.090	0.3731	5.877	(4.896)	(1.1)		(0.7)
$Li^{3+}+Ne\rightarrow Li^{2+}(n=2)+Ne^+$	0.40	0.20	9.019	3.258	0.1470	7.033	(6.250)	(1.1)		(0.9)
$Li^{3+}+Mg\rightarrow Li^{2+}(n=2)+Mg^+$	10.60	3.32	22.934	2.647	0.6820	19.90	(7.957)	(1.1)		(1.9)
$Li^{3+}+Be\rightarrow Li^{2+}(n=2)+Be^+$	5.60	1.81	21.258	2.405	0.9458	41.80	(8.188)	(1.1)		(4.1)
$Li^{3+}+Ar\rightarrow Li^{2+}(n=2)+Ar^+$	1.64	1.17	14.823	2.330	0.9493	90.24	7.719	2.1	1.5	8.0
$Li^{3+}+B\rightarrow Li^{2+}(n=2)+B^+$	3.03	1.53	22.282	2.067	1.5403	98.97	6.074	2.3	1.5	9.0
$Li^{3+}+C\rightarrow Li^{2+}(n=2)+C^+$	1.76	0.82	19.214	2.047	1.5725	139.4	5.958	3.3	2.3	13.0
$Li^{3+}+H\rightarrow Li^{2+}(n=2)+H^+$	0.67	0.00	16.983	2.011	1.6313	204.8	5.750	4.9	3.3	19.0

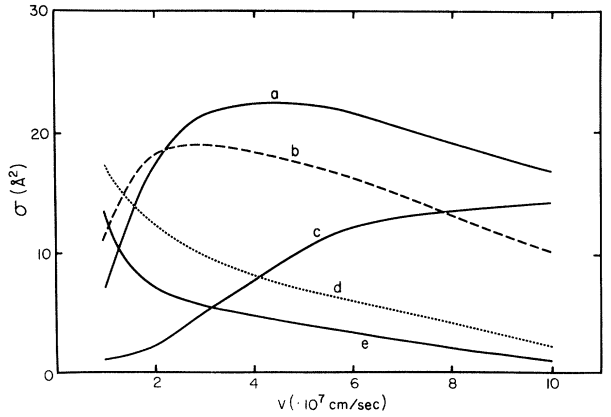

FIG. 1. Cross section σ vs ion velocity v for charge-transfer processes: *a*, $He^{2+}+Be\rightarrow He^{+}(n=2)+Be^{+}$; *b*, $He^{2+}+Ca\rightarrow He^{+}(n=2)+Ca^{+}$; *c*, $He^{2+}+B\rightarrow He^{+}(n=2)+B^{+}$; *d*, $He^{2+}+Li\rightarrow He^{+}(n=2)+Li^{+}$; *e*, $He^{2+}+Cs\rightarrow He^{+}(n=2)+Cs^{+}$.

The starting point of our analysis is Eq. (2.10), the expression for the Landau-Zener cross section. Differentiating both sides of this equation with respect to η/v, we immediately obtain that $v_{\max}$ must satisfy

$$E_2(\eta/v_{\max})-2E_2(2\eta/v_{\max})=0\ , \tag{4.1}$$

where

$$E_2(x)=\int_1^{\infty}\frac{dz}{z^2}\exp(-xz)\ . \tag{4.2}$$

From the table[12] of the exponential integral $E_2(x)$, we find the root of Eq. (4.1),

$$\eta/v_{\max}\cong 0.424\ ,$$

i.e.,

$$v_{\max}\cong\eta/0.424\ . \tag{4.3}$$

Thus $v_{\max}$, the position of the peak, is simply proportional to the parameter η. Substituting Eq. (4.3) into Eq. (2.10), we obtain

$$\sigma_{\max}=4\pi R_c^2[E_3(0.424)-E_3(0.848)]\cong 1.42R_c^2\ . \tag{4.4}$$

Within the Landau-Zener model, $\sigma_{\max}$ depends only on

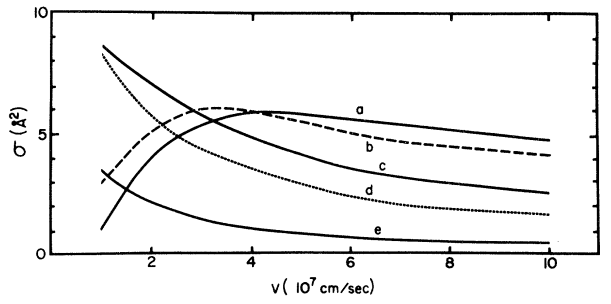

FIG. 2. Cross section σ vs ion velocity v for charge-transfer processes: *a*, $Li^{3+}+H\rightarrow Li^{2+}(n=2)+H^{+}$; *b*, $Li^{3+}+C\rightarrow Li^{2+}(n=2)+C^{+}$; *c*, $Li^{3+}+Be\rightarrow Li^{2+}(n=2)+Be^{+}$; *d*, $Li^{3+}+Mg\rightarrow Li^{2+}(n=2)+Mg^{+}$; *e*, $Li^{3+}+Cs\rightarrow Li^{2+}(n=3)+Cs^{+}$.

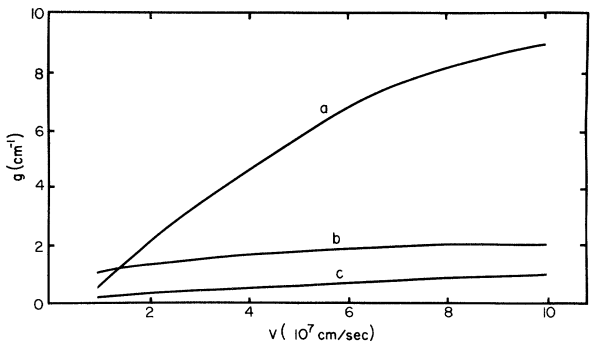

FIG. 3. Gain g vs ion velocity v for charge-transfer processes: *a*, $He^{2+}+Be\rightarrow He^{+}(n=2)+Be^{+}$; *b*, $He^{2+}+Li\rightarrow He^{+}(n=2)+Li^{+}$; *c*, $Li^{3+}+H\rightarrow Li^{2+}(n=2)+H^{+}$.

R_c; different systems with the same crossing distance yield exactly the same peak cross section. This property of the Landau-Zener cross section was already noted by Zwally and Koopman.[9]

In order to find the width of the cross-section curve, we first find the velocity $v_{1/2}$ at which σ becomes one-half of $\sigma_{\max}$. The velocity $v_{1/2}$ must satisfy

$$\sigma_{\max}/2=0.71R_c^2=4\pi R_c^2[E_3(\eta/v_{1/2})-E_3(2\eta/v_{1/2})]\ . \tag{4.5}$$

Equation (4.5) has two roots, $\eta/v_{12}=1.34$ and 0.083, which yield

$$w_L=v_{\max}-\frac{\eta}{1.34}=1.61\eta \tag{4.6a}$$

and

$$w_R=\frac{\eta}{0.083}-v_{\max}=9.69\eta\ . \tag{4.6b}$$

Thus the widths w_L and w_R are simply proportional to η, with w_R roughly six times greater than w_L.

All the values of $\sigma_{\max}$, $v_{\max}$, w_L, and w_R that appear in Tables I and II were taken from our computer calculations. Comparison of these values with those arrived at through Eqs. (4.3), (4.4), and (4.6) showed excellent agreement. (Note, however, that comparison cannot be made on values in the bracket because these values do not represent the "peak" values.) The analysis presented in this section indicates that the trend noted in the previous section, i.e., large cross sections of helium reactions compared with lithium reactions, should not be generalized to heavier-ion reactions. Generally speaking, one would favor a process with large R_c and η which lead to large $\sigma_{\max}$ and width. Such a process can of course be found in heavy-ion reactions too. Perhaps a quick way of judging a given charge-transfer process in connection with the possibility of a short-wavelength laser is to calculate $\sigma_{\max}$, $v_{\max}$, w_L, and w_R using Eqs. (4.3)—(4.6). Before attempting this, however, one may want to ask a fundamental question, i.e., how reliable is the Landau-Zener model itself? In order to investigate this question in more detail, we compare our Landau-Zener cross sections with those obtained with more elaborate numerical methods.

Bransden and Ermolaev[19] have calculated cross sections

for electron capture of He^{2+} from Li into the first excited level ($n=2$) of He^+ using the two-state atomic orbital approach. At $v=4.9\times10^7$, 5.8×10^7, and 8.2×10^7 cm/sec, they obtained $\sigma=11.5$, 10.7, and 10.6 Å^2 compared with our values, $\sigma=6.9$, 6.0, and 4.5 Å^2. The Landau-Zener cross sections are seen to be smaller by a factor of 2. This, however, may not be a good reaction to compare, because it is complicated by the fact that the second excited level ($n=3$) of He^+ is predominantly populated. A more detailed comparison can be done for the Li^{3+}-H reaction. For our comparison we have chosen the unitarized distorted-wave approximation (UDWA) results of Ryufuku and Watanabe,[20] 20-atomic-state calculations of Bransden and Noble,[21] 20-molecular-state calculations of Salin,[22] ten-molecular-state calculations of Kimura and Thorson,[23] and finally experimental data of Seim *et al.*[24] All these data along with our Landau-Zener cross sections appear in Fig. 4. The Landau-Zener cross sections seems to differ rather significantly from other cross sections in that the persistent increase of the cross section toward the high-velocity region seen in other curves is missing in ours. This, however, is at least partly explained by noting that all curves except the curve of Bransden and Noble[21] and ours are total-cross-section curves. At higher velocities other excited levels of Li^{2+} lying higher than the first excited level ($n=2$) will be populated and thus will contribute significantly to the total cross section. The discrepancy seems to lie rather in the low-velocity region ($v\leq5\times10^7$ cm/sec) where the Landau-Zener model yields larger cross sections than all other calculations except for the UDWA results. This is in contrast to findings in the past[5,10] that the Landau-Zener model usually underestimates cross sections. In fact, the discrepancy seen in Fig. 4 is even more serious than it appears because cross sections into the first excited level of Li^{+2} are compared with total cross sections. As pointed out repeatedly in the past, the Landau-Zener model should be used only for a rough estimate of cross sections. The use of the model can perhaps be justified for our preliminary screening of a large number of charge-exchange processes. However, once a small number of more promising candidate processes are selected, more accurate techniques of computing cross sections may have to be employed for a reliable assessment of the performance of possible lasers.

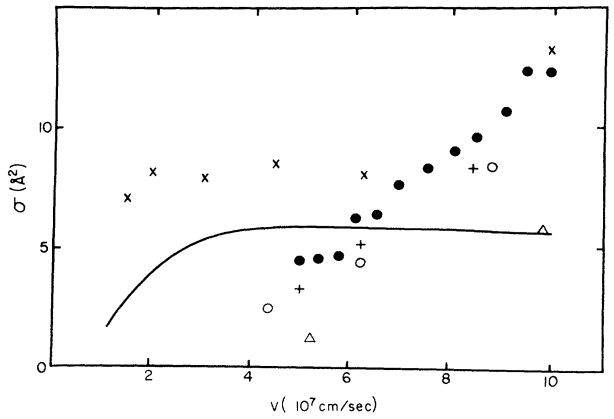

FIG. 4. Cross section σ vs ion velocity v for $Li^{3+}+H\rightarrow Li^{2+}+H^+$. ——, this work (Landau-Zener); ×, Ryufuku and Watanabe (Ref. 20); △, Bransden and Noble (Ref. 21); +, Salin (Ref. 22); ○, Kimura and Thorson (Ref. 23); ●, Seim *et al.* (Ref. 24) (experimental data); —— and △ are cross sections for charge transfer into the first excited level ($n=2$) of Li^{2+}, while others represent total charge-transfer cross sections.

ACKNOWLEDGEMENTS

Acknowledgment is made to the Research Corporation, Oakland University, and to the donors of the Petroleum Research Fund, administered by the American Chemical Society, for support of this research.

[1]A. V. Vinogradov and I. I. Sobel'man, Zh. Eksp. Teor. Fiz. 63, 2113 (1972) [Sov. Phys.—JETP 36, 1115 (1973)].
[2]M. O. Scully, W. H. Louisell, and W. B. McKnight, Opt. Commum. 9, 246 (1973).
[3]L. Landau, Phys. Z. Sowjet Union 2, 46 (1932).
[4]C. Zener, Proc. R. Soc. London, Ser. A 137, 696 (1932).
[5]D. R. Bates, Proc. R. Soc. London, Ser. A 257, 22 (1960); D. R. Bates, H. C. Johnston, and I. Stewart, Proc. Phys. Soc. London 84, 517 (1964).
[6]C. A. Coulson and K. Zalewski, Proc. R. Soc. London, Ser. A 268, 437 (1962).
[7]E. E. Nikitin, Opt. Spectrosc. 13, 431 (1962).
[8]D. R. Bates and B. L. Moiseiwitsch, Proc. Phys. Soc. London, Sect. A 67, 805 (1954).
[9]H. J. Zwally and D. W. Koopman, Phys. Rev. A 2, 1851 (1970).
[10]A. Salop and R. E. Olson, Phys. Rev. A 13, 1312 (1976).
[11]R. E. Olson, F. T. Smith, and E. Bauer, Appl. Opt. 10, 1848 (1971).
[12]*Handbook of Mathematical Functions,* edited by M. Abramowitz and I. A. Stegun (Dover, New York, 1965).
[13]A. Yariv, *Quantum Electronics,* 2nd ed. (Wiley, New York, 1975), Chap. 8.
[14]T. M. Miller and B. Bederson, Adv. At. Mol. Phys. 13, 1 (1977).
[15]*Handbook of Atomic Data, Physical Sciences Data 5,* edited by S. Fraga, K. M. S. Saxena, and J. Karwowski (Elsevier, New York, 1976).
[16]*CRC Handbook of Chemistry and Physics,* 62nd ed., edited by R. C. Weast (CRC, Boca Raton, Florida, 1981).
[17]J. L. Barrett and J. J. Leventhal, Appl. Phys. Lett. 36, 869 (1980).
[18]E. J. Shipsey, L. T. Redmon, J. C. Browne, and R. E. Olson, Phys. Rev. A 18, 1961 (1978).
[19]B. H. Bransden and A. M. Ermolaev, Phys. Lett. 84A, 316 (1981).
[20]H. Ryufuku and T. Watanabe, Phys. Rev. A 19, 1538 (1979).
[21]B. H. Bransden and C. J. Noble, J. Phys. B 15, 451 (1982).
[22]A. Salin, Phys. Lett. 91A, 61 (1982).
[23]M. Kimura and W. R. Thorson, J. Phys. B 16, 1471 (1983).
[24]W. Seim, A. Müller, I. Wirkner-Bott, and E. Salzborn, J. Phys. B 14, 3475 (1981).